MAGNETIC NANOPARTICLES FOR METHYLENE BLUE DYE REMOVAL FROM WASTEWATER

Larisa POPESCU[1], Dorina CREANGA[1], Liviu SACARESCU[2], Marian GRIGORAS[3], Nicoleta LUPU[3]

This report is focused on the wastewater cleaning using a type of magnetic nanoparticles that was rather recently considered for applications in life sciences. It is gallic acid/magnetite that we prepared and characterized for the study of methylene blue removing from dye loaded waters. The magnetic nanoparticles were let to interact with pollutant molecules under UVC exposure. Optimization of polluting molecule/magnetic nanoparticle ratio was carried out by electronic absorption spectrum and resulted in total degrading of 0.1 μM methylene blue in 120 minutes of UVC exposure in the presence of 4 gL^{-1} magnetic nanoparticles.

Keywords: Gallic Acid/Magnetite, Transmission Electron Microscopy, X-Ray Diffraction, Magnetometry, Blue Methylene Pollutant.

1. Introduction

The applications of magnetic nanoparticles (MNPs) in life sciences were first dedicated to experimental biomedicine [1-5], but next the scientists' attention was attired by environmental issues. On a side there is the interest for MNP toxicity [6-7] while, on the other side, some benefits of MNPs were taken into consideration, related to their interaction with environment risk factors, mainly wastewater [8-9]. Some studies reported the usability of MNPs in removal pollutants like: phenolic compounds [10-11] dyes like methylene blue [12-14], or methyl orange [15-17]. During last years the developing of gallic acid/iron oxide magnetic nanoparticles could be underlined, in the first place for drug delivery [18] and then for removal of specific toxic components from industrial waters [19]; cleaning of pharmaceutical wastewater loaded with anti-inflammatory drugs was discussed in [19] and microorganism inactivation was presented in [20].

We also studied iron oxide magnetic nanoparticles from the view point of their properties when stabilized in the form of stable aqueous suspension [21-23] and aiming some applications in physics [24] and life sciences [25].

[1] Alexandu Ioan Cuza, University Iasi, Physics Faculty, e-mail: dorina.emilia.creanga@gmail.com
[2] P. Poni Institute of Macromolecular Chemistry, Iasi
[3] Iasi National Institute of Research and Development for Technical Physics

2. Experimental

2.1. Nanosized magnetic powder synthesis

Massart's basic procedure [26] was applied starting with synthesis of the ferrophase by mixing together the precursor reagents, ferrous chloride tetrahydrate $FeCl_2 \times 4H_2O$) and ferric chloride hexahydrate ($FeCl_3 \times 6H_2O$) under normal atmospheric conditions, in the presence of a strong alkaline precipitation agent (1.7M NaOH). The chemicals used in the study were high-purity analytical reagents purchased from Merck (Sigma-Aldrich) and used without additional purification; the deionized water (18.2 MΩ/cm) used throughout the whole experiment was obtained using Barnstead EasyPureII water purification system.

2.2. Gallic acid supply for nanosized powder capping

Magnetic nanoparticles (MNP) were coated with gallic acid (GA) by continuous mechanical stirring at high temperature, in concentration of 0.6 mM GA/g magnetite, adapted after [27], and repeatedly washed with ultrapure water, in order to remove impurities and excess coating molecules. These way Fe_3O_4@GA nanoparticles were prepared.

2.3. Physical properties characterization

TEM (Transmission Electron Microscopy) investigation was done using Hitachi High-Tech HT7700 device working at 120 kV with 1 nm resolution.

X-ray diffractometry was applied for crystalinity study using Shimadzu 6000 X-ray diffractometer device with Cu-K_α radiation at λ = 1.5406 Å on the range of 2θ from 20 to 80 degrees.

Magnetic properties were evidenced at room temperature by means of magnetization measurements using Vibrating Sample Magnetometer System (MicroMag model 2900/3900) device on freshly prepared Fe_3O_4@GA suspension.

The hydrodynamic diameter distribution and Zeta potential of ferrophase aqueous suspension were estimated by Dynamic Light Scattering (DLS) with Zetasizer Ultra device (Malvern Instruments), after the magnetic materials were dried under vacuum at 90 °C for 6 h, and resuspended in ultrapure water as diluted concentration samples.

2.4. Methylene blue spectral characterization

Quantum-mechanical modeling of methylene blue (MB) electronic absorption spectrum (EAS) was carried out with commercially available software

HyperChem. Spectral properties of MB aqueous solution were studied by means of Shimadzu 1700 UV–Vis spectrophotometer (using 1 cm quartz cuvette) that allowed spectral monitoring of the environmental application.

2.5. Wastewater samples

The MB aqueous solutions were prepared by adding an appropriate amount of methylene blue ($C_{16}H_{18}CIN_3S$,) in ultrapure water in order to reach the studied concentration (1 μM and 1.5 μM).

Fe_3O_4@GA nanoparticle suspensions were dried under vacuum at 90 °C for 6 hours; two Fe_3O_4@GA concentrations, 2.0 and respectively 4.0 gL^{-1} were tested. The experiments were performed at room temperature under mechanical stirring (1200 rpm). The UV exposure was carried out using UVC lamps (UV Flow Activa HF 120) with 30 Wm^{-2} intensity. In all experiments a total reaction volume of 10 mL was irradiated, the sample vessel being placed at 20 cm under the radiation source with exposed surface of 12.57 cm^2.

The light absorbance curve was recorded at different times (T=0; 30; 60 and 120 min) during irradiation; before absorbance recording the nanoparticles used in the study were withdrawn from their action medium by magnetic decantation. Since absorbent molecule concentration is directly proportional to sample light extinction – in accord with to Beer-Lambert law, degrading rate could be assessed with the relation: MB degradation (%)=$(A_f-A_0)/A_f \times 100\%$, where A_0 corresponds to the light extinction of MB initial concentration and A_f to the concentration of MB after degrading.

3. Results and discussion

3.1. Microstructural and magnetic properties

TEM images (Fig. 1) of Fe_3O_4@GA nanoparticles showed rather regular geometric structures, mostly quasi-spherical, with average nanoparticle diameter (ImageJ software), D_{TEM}, of about 9.5 nm (Table 1). XRD recording (Fig. 2a) evidenced the crystalline nature of synthesized MNPs; inverse spinel structure with all characteristic magnetite peaks according to ASTM Card 11-614 [28] were recorded with no additional peaks and no amorphous fraction. Measured positions of diffraction peaks were close to literature standard values (ASTM Card 11-614) of magnetite powder: (220), (311), (400), (422), (511), (440) and (533) in the 2θ range of 20–80 degrees. The crystallite size was calculated from the strongest peak (311), using Scherrer's formula [29].

VSM recording (Fig. 2b) reveals the superparamagnetic properties of Fe_3O_4@GA nanoparticle aqueous suspension with saturation magnetization of 14.5 emu/cm^3, presenting very thin hysteresis loop (coercitive field in Table 1).

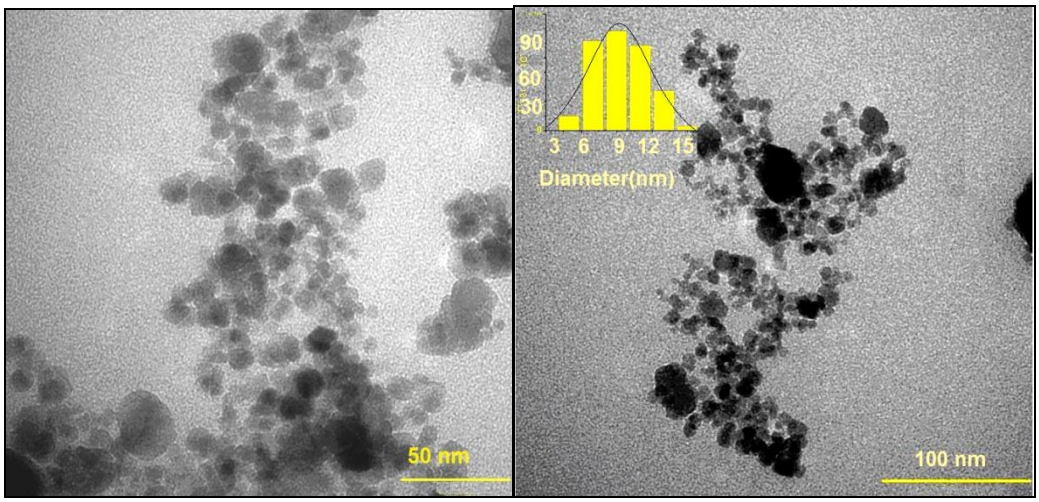

Fig. 1. Transmission Electron Microscopy images for Fe_3O_4@GA nanoparticles

The MNPs largest magnetic diameter (D_M - Table 1) was calculated from Langevin's theory:

$$D_M^3 = \frac{18 k_B T}{\pi \mu_0 M_s m_s} \left(\frac{dM}{dH}\right)_{H \to 0} \tag{1}$$

where k_B is Boltzmann's constant, T is the absolute temperature, M_s is saturation magnetization of MNP-coated powder, μ_0 is vacuum magnetic permeability, m_s=0.48x10^6 A/m (bulk magnetite saturation magnetization, [28]) and *(dM/dH)* is the slope in the graph origin (for *H*-magnetic field intensity-near zero).

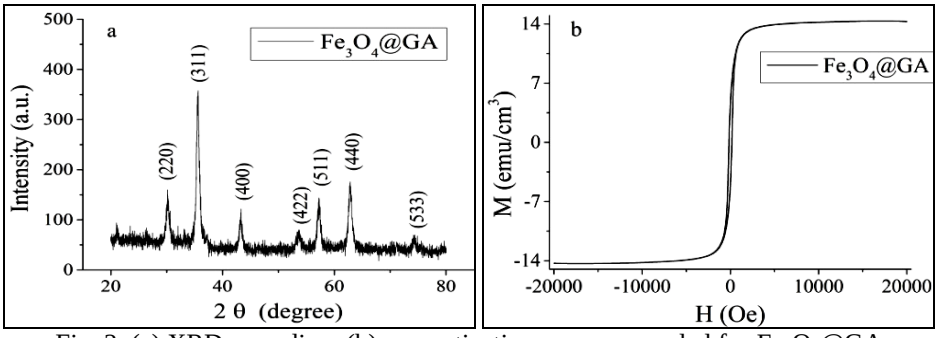

Fig. 2. (a) XRD recording; (b) magnetization curves recorded for Fe_3O_4@GA

Table 1 summarizes the microstructural and magnetic properties of the analyzed nanoparticles, namely Fe_3O_4@GA.

As shown in Fig. 3a, DLS investigation provided the size distribution profile, with mean hydrodynamic diameter D_H of 660.9 nm. Zeta potential,

resulted from surface charge double layer effect, can greatly influence particle stability in suspension through the electrostatic repulsion between particles.

Table 1.

The microstructural and magnetic parameters of gallic acid coated magnetite nanoparticles used in the study

	D_{TEM} (nm)	D_{311} (nm)	D_M (nm)	H_{ci} (Oe)	M_s (emu/cm^3)	D_H (nm)	V (mV)
Fe_3O_4@GA	9.5	8.0	8.87	158.5	14.5	660.9	-23.93

As shown in Fig. 3b, the Fe_3O_4@GA nanoparticles had a Zeta potential *V*, of -23.93 mV.

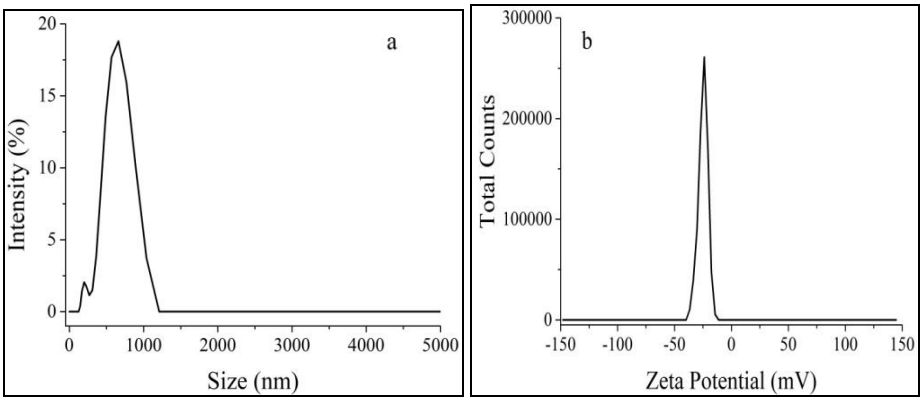

Fig. 3. (a) The size distribution; (b) Zeta potential of Fe_3O_4@GA nanoparticles

According to [30] physical stability of nanosuspensions stabilized by electrostatic repulsion theoretically requires Zeta potential threshold of ±30 mV; so the studied Fe_3O_4@GA aqueous sample is close to theoretical threshold, thus additional stirring was carried out during UVC exposure to ensure suspension homogeneity.

3.2. Methylene blue molecule study

Optimized MB structure was released with some general and specific parameters (electric dipole, partition coefficient, boundary molecular orbital energies) using mathematical modeling method with PM3 (Parametric Method 3, based on parametrization by optimization of one-center electron repulsion integrals) (Table 2). The modeled electronic absorption spectrum (EAS) as transitions between HOMO (Highest Occupied Molecular Orbital) and LUMO

(Lowest Unoccupied Molecular Orbital) levels, in Fig. 4a is represented while the experimentally recorded spectrum for MB in water in Fig. 4b can be seen. Log P parameter positive value reflect limited solubility of MB in water compared to hydrocarbons.

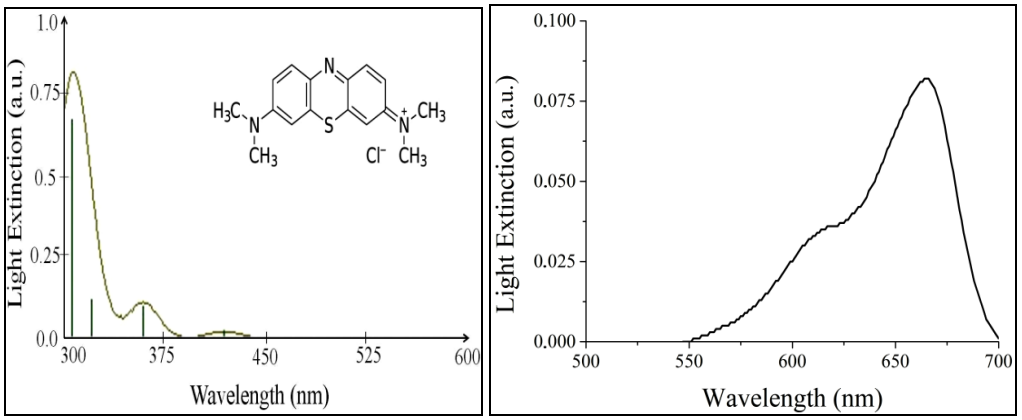

Fig. 4. (a) Modeled EAS of isolated MB (b) Recorded EAS of MB in water solution

The differences of EAS peak positions and relative intensities are explained mainly by the solvent effect, in this case the red shift (toward higher wavelength) and reversal of peak relative intensities.

Table 2

Methylene blue parameters

MB ($C_{16}H_{18}ClN_3S$)	Dipole moment (D)	HOMO energy (eV)	LUMO energy (eV)	Refractivity (Å^3)	Polarizability (Å^3)	LogP
	0.78	-7.5222	-1.9571	94.11	38.61	4.1
Spectral properties	Isolated molecule EAS (nm)			EAS of MB in water (nm)		
	305		355	615	665	

The solute-solvent intermolecular interactions are expected to occur due to electric dipoles of water. Quantum mechanics estimations resulted in 1.85 D for water and respectively 0.78 D for MB - the two molecules coexisting within the solutions studied in this research.

To monitor the concentration changes of methylene blue dye the 665 nm absorption maximum was selected. In Fig. 5 the UV exposure effect is presented for the tested time durations (30; 60; 120 min) with up to 46% diminution of EAS maximum intensity in the case of 1.0 μM concentration of MB. The increase to 1.5 μM of MB concentration has resulted in the saturation of UV exposure effect

(with about 30% diminution of EAS intensity at 665 nm) from 30 min to 120 min exposure time (Fig. 5 b).

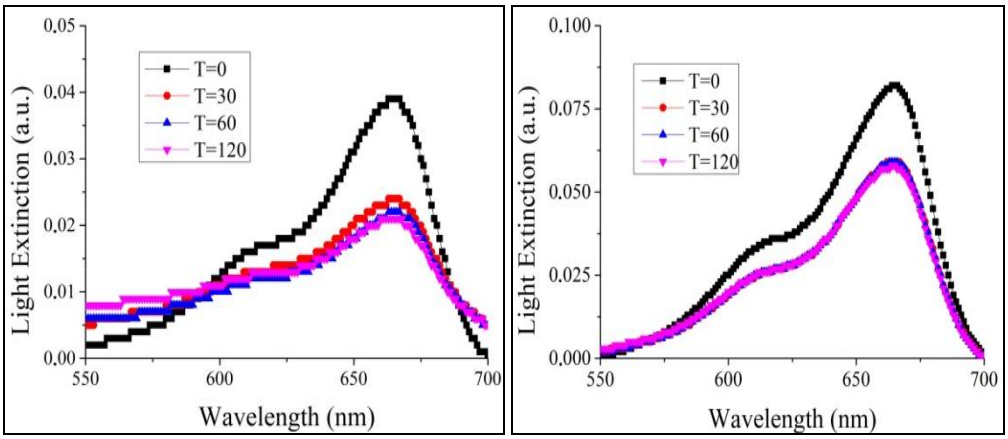

Fig. 5. Photodegradation of MB for three UV exposure time durations of 30 min, 60 min, 120 min (1.0 μM MB concentration – left; 1.5 μM MB concentration - right)

According to [31] in the presence of UV light, MB can absorb light energy, which could lead to the self-decomposition with formation of extremely energetic and active singlet and triplet species. Those can react with the available oxygen and form reactive oxidation species (ROS) like superoxide, peroxide and hydroxyl radicals.

Due to their reactivity, ROS can degrade and mineralize the MB molecule, leading to the decrease of the MB concentration from the solution. Other authors [32] evidenced by EPR various paramagnetic MB species resulted from photolysis, including oxidized and reduced ones as well as dimmers and trimers – with absorption peak at about 615 nm, co-existing to initial monomers – with the main absorption peak at 665 nm. Since in Fig. 5 the relative intensity of 665 nm peak (relatively to 615 nm peak intensity) has decreased after UVC irradiation for 120 min (from about 2.5 to less than 1.7), we might suppose that UV light effect is underlying this changing.

3.3. MB photodegrading with Fe_3O_4@GA nanoparticles

Two MNPs concentrations that were tested in the aqueous MB samples under UV exposure were of 2.0 and 4.0 gL^{-1}. Compared to photodegradation under UV exposure only, the addition of either 2 gL^{-1}or 4 gL^{-1} of Fe_3O_4@GA nanoparticles, has caused the intensification of MB degradation for both concentrations (1.0 μM and 1.5 μM MB).

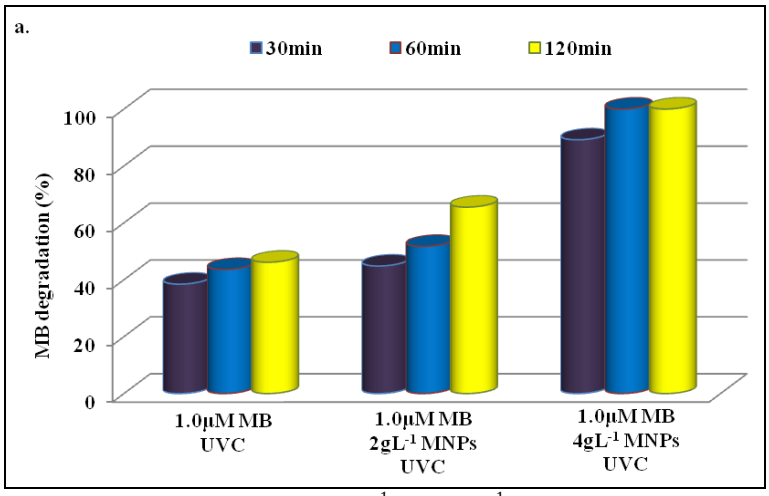

Fig. 6 a. Degradation of 1.0 µM MB with $2gL^{-1}$ and 4 gL^{-1} magnetic nanoparticles under UVC exposure

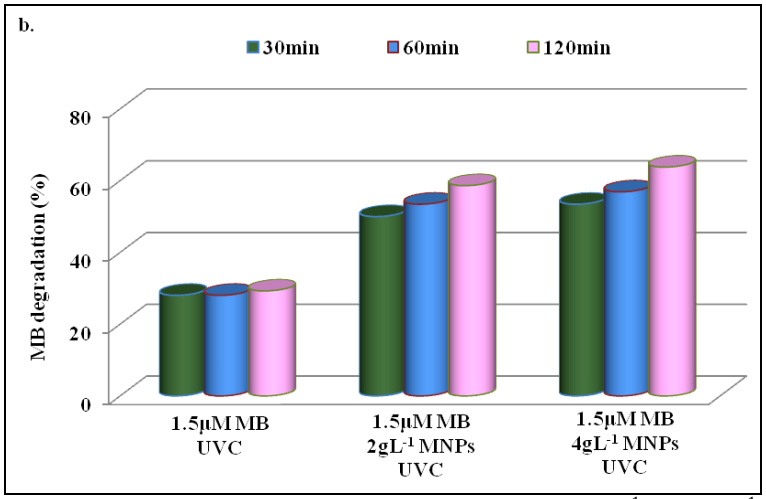

Fig. 6b. Degradation of 1.5 µM MB under UVC exposure with $2gL^{-1}$ and 4 gL^{-1} magnetic nanoparticles

(i)The effect of magnetic nanoparticles supply on the methylene blue degradation is shown in Fig. 6a, for 4.0 gL^{-1} Fe_3O_4@GA nanoparticles, that has induced complete (100%) degradation of 1.0 µM MB after about 60 min UV exposure, while 65.5% MB degrading in 1.0 µM MB sample was obtained with 2.0 gL^{-1} Fe_3O_4@GA nanoparticles for 120 min exposure to UV beam (standard deviation of about 3%);

(ii) for higher MB concentration, of 1.5 µM, the magnetic nanoparticles effect was lowered: no more than 63.8% intensity diminution of 665 nm EAS band was recorded for 4.0 gL^{-1} Fe_3O_4@GA nanoparticles (for longest UV

exposure time, of 120 min) and respectively 58.6% for 2.0 gL^{-1} Fe_3O_4@GA nanoparticles. According to [33-35] the mechanism of interaction between magnetic nanoparticles and MB is mainly the adsorption of dye molecules at the surface of ferrophase grains.

The results could be interpreted as corroborated effects of UV rays, that induce MB photolysis, and magnetic nanoparticles, that adsorb them at the surface modified with coating molecules. The dye molecule association in reversible dimmers/trimers also could influence the efficiency of MB degradation from loaded waters. New experiments could be developed based on similar experimental design to search for catalytic effect of metal ions released from the surface of gallic acid/magnetite nanoparticles in the presence as well as in the lack of UV induced photolysis.

4. Conclusion

Wastewater loading with methylene blue dye could be adjusted by treating them with energetic light beam based on photolytic effect, able to destabilize pollutant molecules; the supply with magnetic nanoparticles could further led to collecting of degraded pollutant species by adsorption at their surface up to completely cleaning.

The above presented study showed that UVC exposure alone could degrade up to 30% or 46% for the MB concentrations tested in this experiment.

When gallic acid/magnetite nanoparticles were additionally involved, then the degradation percentage increased remarkably reaching 100% for optimal combination of Fe_3O_4@GA nanoparticles and MB concentrations.

Deeper insight in the mechanisms of dye pollutant decomposition under UV rays as well as by supplying magnetic nanoparticles is planned to be obtained from testing new variants of experimental conditions and reaction parameters to shape the possible application to large wastewater volumes.

Acknowledgement: this study was supported by RO-JINR project 04-4-1121/2017-2020

R E F E R E N C E S

[1]. *E. Illés, M. Szekeres, E. Kupcsik, I.Y. Tóth, and K. Farkas*, "PEGylation of surfacted magnetite core-shell nanoparticles for biomedical application", in Colloids and Surfaces A, **vol. 460**, 2014, pp. 429-440.

[2]. *S. Mornet, S. Vasseur, F. Grasset, E. Duguet*, "Magnetic nanoparticle design for medical diagnosis and therapy", in Journal of Materials Chemistry, **vol. 14**, 2004, pp. 2161-2175.

[3]. *J. E. Rosen, L. Chan, D.B. Shieh, and F. X. Gu*, "Iron oxide nanoparticles for targeted cancer imaging and diagnostics", in Nanomedicine: Nanotechnology, Biology and Medicine, **vol. 8**, 2012, pp. 275-290.

[4]. *M. Mahdavi, M. B. Ahmad, M. J. Haron, F. Namvar, B. Nadi, M. Z. A. Rahman, and J. Amin,* "Synthesis, surface modification and characterisation of biocompatible magnetic iron oxide nanoparticles for biomedical applications", in Molecules, **vol. 18**, 2013, pp. 7533-7548.

[5]. *A. C. Silva, T. R. Oliveira, J. B. Mamani, S. M. Malheiros, L. Malavolta, L. F. Pavon, T. T. Sibov, E. Jr. Amaro, A. Tannús, E. L. Vidoto, M. J. Martins, R. S. Santos, and L. F. Gamarra*, "Application of hyperthermia induced by superparamagnetic iron oxide nanoparticles in glioma treatment" in International Journal of Nanomedicine, **vol. 6**, 2011, pp. 591–603.

[6]. *M. Racuciu, and D. Creanga*, "Magnetite/tartaric acid nanosystems for experimental study of bioeffects on Zea mays growth", in Romanian Journal of Physics, **vol. 62** (3-4), 2017, art. 804.

[7]. *L. Oprica, C. Nadejde, M. Andries, E. Puscasu, D. Creanga, and M. Balasoiu*, "Magnetic contamination of environment–laboratory simulation of mixed iron oxides impact on microorganism cells", in Environmental Engineering and Management Journal, **vol. 14(**3), 2015, pp. 581-586.

[8]. *C. Nadejde, M. Neamtu, R. J. Schneider, V. D. Hodoroaba, G. Ababei, and U. Panne*, "Catalytical degradation of relevant pollutants from waters using magnetic nanocatalysts", in Applied Surface Science, v**ol. 352**, 2015, pp. 42-48.

[9]. *X. Huang, C. Xu, J. Ma, and F. Chen*, "Ionothermal synthesis of Cu-doped Fe_3O_4 magnetic nanoparticles with enhanced peroxidase-like activity for organic wastewater treatment", in Advanced Powder Technology, **vol. 29**, 2018, pp. 796-803.

[10]. *W. Wang, Y. Liu, T. Li, and M. Zhou,* "Heterogeneous Fenton catalytic degradation of phenol based on controlled release of magnetic nanoparticles", in Chemical Engineering Journal, **vol. 242**, 2014, pp. 1-9.

[11]. *C. Nadejde, M. Neamtu, V.D. Hodoroaba, R. J. Schneider, G. Ababei, and U. Panne*, "Hybrid iron-based core–shell magnetic catalysts for fast degradation of bisphenol A in aqueous systems", in Chemical Engineering Journal, **vol. 302**, 2016, pp. 587-594.

[12]. *X. Zhang, P. Zhang, Z. Wu, L. Zhang, G. Zeng, C. Zhou,* "Adsorption of methylene blue onto humic acid-coated Fe_3O_4 nanoparticles, Colloids and Surfaces A: Physicochemical and Engineering Aspects, **vol. 435,** 2013, pp. 85-90.

[13]. *Y. M. Li, X. Miao, Z. G. Wei, J. Cui,S. Y. Li, R. M. Han, Y. Zhang, and W. Wei*, "Iron-Tannic Acid Nanocomplexes: Facile Synthesis And Application For Removal Of Methylene Blue from Aqueous Solution", in Digest Journal of Nanomaterials and Biostructures, **Vol. 11**, 2016, pp. 1045-1061.

[14]. *K. K. Singh, K. K. Senapati, and K. C. Sarm*, "Synthesis of superparamagnetic Fe_3O_4 nanoparticles coated with green tea polyphenols and their use for removal of dye pollutant from aqueous solution", in Journal of Environmental Chemical Engineering, **vol. 5**, 2017, pp. 2214-222.

[15]. *D. Zhao, J. Cheng, and J. Chen*, "One-step synthesis of bentonite-supported nanoscale Fe/Ni bimetals for rapid degradation of methyl orange in water", in Environmental Chemistry Letters, **vol. 12**, 2014, pp. 461-466.

[16]. *M. H. Do, N. H. Phan, T. D. Nguyen, T. T. S. Pham, V. K. Nguyen, T. T. T. Vu, and T. K. P. Nguyen,* "Activated carbon/Fe_3O_4 nanoparticle composite: Fabrication, methyl orange removal and regeneration by hydrogen peroxide", in Chemosphere, **vol. 85**, 2011, pp. 1269-1276.

[17]. *H. Sarvari, E. K. Goharshadi, S. Samiee, and N. Ashraf*, "Removal of Methyl Orange from Aqueous Solutions by Ferromagnetic Fe/Ni Nanoparticles", in Physical Chemistry Research, **vol. 6**, 2018, pp. 433-446.

[18]. *D. Dorniani, M.Z. Hussei, A.U. Kura, S. Fakurazi, A. Shaari, and Z. Ahmad*, "Preparation of Fe_3O_4 magnetic nanoparticles coated with gallic acid for drug delivery", in International Journal of Nanomedicine, **vol. 7**, 2014, pp. 5745-5755.

[19]. *A. H. Nadim, M. A. Al-Ghobashy, M. Nebsena, and M. A. Shehata,* "Gallic acid magnetic nanoparticles for photocatalytic degradation of meloxicam: synthesis, characterization and application to pharmaceutical wastewater treatment", in RSA Advances, **vol. 5**, 2015, pp. 104981-104990.

[20]. *S. T. Shah, W. A. Yehye, O. Saad, K. Simarani, Z. Z. Chowdhury, and A. A. Alhadi*, "Surface functionalization of iron oxide nanoparticles with gallic acid as potential antioxidant and antimicrobial agents", in Nanomaterials, **vol. 7** (10), 2017, art. 306.

[21]. *G. Tiriba, M. Balasoiu, E. Puscasu, L. Sacarescu, C. Stan, and D. Creanga,* "Microstructural characterization of Co-doped iron oxide nanoparticles", in UPB Scientific Bulletin, Series A: Applied Mathematics and Physics, **vol.79** (4), 2017, pp. 327-336.

[22]. *C. Nadejde, E. Puscasu, F. Brinza, L. Ursu, D. Creanga, and C. Stan*, "Preparation of soft magnetic materials and characterization with investigation methods for fluid samples", in UPB Scientific Bulletin, Series A: Applied Mathematics and Physics, **vol. 77**(2), 2015, pp. 277-284.

[23]. *M. Racuciu, D. Creanga, and C. Nadejde***,** "Comparison among the physical properties of various suspensions of magnetite nanoparticles stabilized in water using different organic shells", in UPB Scientific Bulletin, Series A: Applied Mathematics and Physics, **vol. 75**(3)**,** 2013, pp. 209-216.

[24]. *C. Cîrtoaje, E. Petrescu, C. Stan, and Dorina Creang,* "Ferromagnetic nanoparticles suspensions in twisted nematic" in Physica E: Low-dimensional Systems and Nanostructures, **vol.79**, 2016, pp. 38-43.

[25]. *I. Bodale, M. Oprisan, C. Stan, F. Tufescu, M. Racuciu, D. Creanga, and M. Balasoiu,* "Nanotechnological application based on $CoFe_2O_4$ nanoparticles and electromagnetic exposure on agrotechnical plant growth", in 3rd International Conference on Nanotechnologies and Biomedical Engineering, **vol. 55**, 2016, pp. 153-156.

[26]. *R. Massart*, "Preparation of aqueous magnetic liquids in alkaline and acidic media", in IEEE Transactions Magnetics, **vol. 17**, 1981, pp. 1247–1248.

[27]. *M. Szekeres, E. Illés, C. Janko, K. Farkas, I. Y. Tóth, D. Nesztor, I. Zupkó, I. Földesi, C. Alexiou, and E. Tombácz*, "Hemocompatibility and biomedical potential of poly(gallic acid) coated iron oxide nanoparticles for theranostic use", in Journal of Nanomedicine and Nanotechnology, **vol. 5**(6), 2015, art. 1000252.

[28]. *H. E. Swanson and E. Tatge*, "Standard X-ray diffraction powder patterns", in Government Printing Office, Washington, 1967.

[29]. *A. Patterson*, "The Scherrer Formula for X-Ray Particle Size Determination", Physical Reviews, **vol. 56** (10), 1939, pp. 978–982.

[30]. *R.E. Rosensweig*, Ferrohydrodynamics, in Cambridge University Press, Cambridge, 1985.

[31]. *R. H. Müller, C. Jacobs, and O. Kayser*, "Nanosuspensions as particulate drug formulations in therapy rationale for development and what we can expect for the future", in Advanced Drug Delivery Reviews, **vol. 47**, 2001, pp. 3–19.

[32]. *S. Shahabuddin, N. M. Sarih, F. H. Ismail, M. M. Shahidb and N. M. Huang*, "Synthesis of chitosan grafted-polyaniline/Co3O4 nanocube nanocomposites and their photocatalytic activity toward methylene blue dye degradation", in RSC Advances, **vol. 5**, 2015, pp. 83857–83867.

[33]. *M. Contineanu, C. Bercu, I. Contineanu, and A. Neacşu*, "A chemical and photochemical study of radicalic species formed in methylene blue acidic and basic aqueous solutions", in Annals of Bucharest University, Chemistry series, **vol. 18**(2), 2009, pp. 29 – 37.

[34]. *E. Alzahrani***,** "Gum Arabic-Coated Magnetic Nanoparticles for methylene blue removal", in International Journal of Innovative Research in Science, Engineering and Technology, **vol. 3**(8), 2014, pp. 15118-15129.

[35]. *W. Zeng, Y. G. Liu, X. J. Hu, S. B. Liu, G. M. Zeng, B. H. Zheng, L. H. Jiang, F. Y. Guo, Y. Ding, and Y. Xu*, "Decontamination of methylene blue from aqueous solution by magnetic chitosan lignosulfonate grafted with graphene oxide: effects of environmental conditions and surfactant", in RSC Advances, **vol.** 6, 2016, pp. 19298-19307.

[36]. *Y. Hua, J. Xiao, Q. Zhang, C. Cui, and C. Wang*, "Facile synthesis of surface-functionalized magnetic nanocomposites for effectively selective adsorption of cationic dyes" in Nanoscale Research Letters, **vol. 13**, 2018, pp. 1-9.